https://doi.org/10.17221/4/2024-CJFS

Green synthesis, characterisation, and antibacterial activity of silver nanoparticles obtained from *Salvia officinalis* extract

*Tuğçe Özeşer, Nural Karagözlü**

Food Engineering Department, Engineering Faculty, Manisa Celal Bayar University, Manisa, Türkiye

**Corresponding author: nural.karagozlu@cbu.edu.tr*

Citation: Özeşer T., Karagözlü N. (2024): Green synthesis, characterisation, and antibacterial activity of silver nanoparticles obtained from *Salvia officinalis* extract. Czech J. Food Sci., 42: 163–173.

Abstract: The present study investigated the properties and antimicrobial activity of silver nanoparticles synthesised through a green method using *Salvia officinalis*. Extracts were obtained from sage at two different temperatures, and these extracts were then used to synthesise silver nanoparticles through a reaction with $AgNO_3$. The characteristics of resulting silver nanoparticles and their antimicrobial effects on foodborne pathogenic bacteria were examined. During the synthesis, the colour of the silver nanoparticle solution changed from yellow to dark brown, and a significant absorbance peak was observed at 360 nm. The sizes of the synthesised silver nanoparticles were found to be 53.77 and 57.08 nm for the two different extraction temperatures, respectively. The nanoparticles exhibited spherical-rod shapes with silver contents of 83.91% and 84.38% and crystal sizes of 37.15 nm and 34.81 nm, corresponding to the two temperatures. The reduction of silver ions involved functional groups like C=C or C=O. The antimicrobial activity of the synthesised silver nanoparticles was evaluated at concentrations of 10 and 25 $mg \cdot mL^{-1}$ using the paper disc method against several foodborne pathogenic bacteria. Notably, the sage extract displayed antimicrobial efficacy against *Salmonella* Typhi, *Listeria monocytogenes*, and *Staphylococcus aureus*. However, no significant antimicrobial effect was observed against *Escherichia coli* O157:H7.

Keywords: AgNP; antimicrobial effect; biological method; foodborne pathogen; sage

Nanoparticles form through the combination and crystallisation of atoms within the range of 1–100 nm. In recent times, significant research has been directed towards the biological-green synthesis method. In this innovative approach, nanoparticles are synthesised through reactions involving extracts derived from plants and microorganisms, along with metal salts. Unlike conventional techniques, the biological method offers distinct advantages such as cost-effectiveness, accessibility, and applicability in food and healthcare, primarily attributed to its non-toxic nature (Kumar et al. 2019; Nazri and Sapawe 2020). Considering the general explanation of the antimicrobial activity of silver nanoparticles (AgNPs), it can be observed that biologically synthesised nanoparticles adhere to bacterial cells and subsequently damage the cell membrane by weakening it. Upon penetration through the cell membrane, AgNPs stimulate reactive oxygen species (ROS) production, leading to protein and antioxidant deterioration within the bacterial cell. This process results in DNA damage, glutathione reduction, heightened oxidative stress, and a subsequent reduction in adenosine triphosphate (ATP) levels. Consequently, the proliferation of bacterial cells is impeded, ultimately inducing cell death, as demonstrated by Hernández-Morales et al. (2019).

Supported by the Manisa Celal Bayar University Research Projects Management Unit (Project No. 2021-033).

https://doi.org/10.17221/4/2024-CJFS

Sage (*Salvia officinalis*) is a shrub-shaped plant belonging to the *Lamiaceae* family within the *Lamiales* order. It is distributed in various species across America, Asia, and Mediterranean countries. Various spices and herbs, such as *S. officinalis*, can be utilised in nanoparticle synthesis through biological methods. *S. officinalis* is a plant species containing crucial phenolic components in its structure. It encompasses diverse phenolic compounds, including gallic acid, kaempferol, naringin, quercetin, glycosides, apigenin, flavone, rosmaric acid, catechin, and caffeic acid, within its extract. Vitamins, proteins, amino acids, and polysaccharides found in these plants facilitate the formation of nanoparticles, while alkaloids, terpenes, glycosides, and flavonoids are involved in the reduction of silver ions and the stability of nanoparticles (Paiva-Santos et al. 2021; Takçı et al. 2023).

The present study synthesised nanoparticles from extracts of *S. officinalis* obtained at two different extraction temperatures: 20 and 60 °C. The properties of the synthesised nanoparticles, including size, shape, phenolic group content, element composition, and crystal structure, were determined. Simultaneously, the antimicrobial effects of AgNPs on foodborne pathogenic bacteria such as *Staphylococcus aureus, Listeria monocytogenes, Salmonella* Typhi, and *Escherichia coli* O157:H7 were investigated.

MATERIAL AND METHOD

Plant material. The sage plant was supplied dried from Kütaş Tarım Ürünleri Dış Tic. ve San. A.Ş. company. Following the grinding process, ground sage was stored in glass jars in a cool environment. *Staphylococcus aureus* (ATCC 12600), *Listeria monocytogenes* (ATCC 7644), *Salmonella* Typhi (ATCC 14028), and *Escherichia coli* O157:H7 (ATCC 25922) bacteria cultures were sourced from the Department of Dairy Technology, Faculty of Agriculture, Ege University.

Preparation of *S. officinalis* extract. The sample was processed using room temperature (20 °C) and 60 °C. A quantity of 10 g of sage plant material was employed, to which 100 mL of distilled water was added. After thoroughly mixing in a shaking incubator at 130 revolutions per minute (rpm) for 20 min at both specified temperatures, the resultant extract was filtrated through Whatman No. 1 filter paper. Following filtration, centrifugation was performed at 4 100 rpm for 10 min using a NÜVE NF 800 R centrifuge (Türkiye). The upper phase of the centrifuged extract was collected, producing the extract designated for employment in the forthcoming study.

Silver nanoparticle synthesis. To synthesise AgNP, a solution of 90 mL 1 mM $AgNO_3$ (423952; Carlo Erba, Italy) was combined with 10 mL of sage extract. The mixture was agitated at 130 rpm and ambient temperature for 20 min. This process was carried out in a light-proof shaking incubator. After the mixing phase, the solution was placed in a dark environment and allowed to stand for 1 h. This led to an observable colour transition from yellow to dark brown. To impurify the AgNPs, the solution was centrifuged at 4 100 rpm for 25 min, the top phase was discarded, and the washing process was performed by adding pure water to the remaining part. After the washing process was repeated several times, the AgNPs were taken into Petri dishes, dried in a vacuum oven at 65 °C, and kept in a dark environment under room conditions, ready for use in the analysis.

Characterisation of synthesised silver nanoparticles. In the synthesis of AgNPs, spectral analysis was conducted to observe the colour change resulting from the reduction of silver. Spectrophotometric analysis of the extract and nanoparticles was carried out using a spectrophotometer (UV-1601 UV-Vis; Shimadzu, Japan), covering a wavelength range of 200 to 1 000 nm. The acquisition of spectra was performed against pure water at a moderate speed. Scanning electron microscopy (SEM) (Gemini 500; Zeiss, Germany) was employed to determine the morphological structure of the AgNPs. At the same time, energy-dispersive X-ray spectroscopy (EDX) was utilised to confirm the presence of silver and other elements (Gemini 500; Zeiss, Germany). The SEM analysis utilised carbon tape, and the gold coating was applied under vacuum conditions to enhance nanoparticle conductivity. ImageJ software (version 1.53t) determined particle size, and a histogram graph was generated using the Statistical Package for the Social Sciences program (IBM SPSS Statistics, version 27). The synthesis of AgNPs involves the reduction of silver using functional components from plant extracts. fourier transform infrared (FTIR) analysis was conducted using the Thermo Scientific Nicolet IS20 instrument (Thermo Fisher Scientific, USA) to identify the functional groups responsible for this reduction. The study encompassed the 4 000 to 400 cm^{-1} range to analyse functional groups.

To determine the crystal structure and size of the compounds present in the AgNPs, the analyses were conducted using the PANalytical EMPYREAN-branded X-ray diffraction (XRD) instrument (United Kingdom) over a $5 \leq 2\theta \geq 85°$ (2θ – angle between transmitted beam and reflected beam). The nanoparti-

https://doi.org/10.17221/4/2024-CJFS

cles' crystal size was determined by utilising the Debye-Scherrer Equation 1:

$$D = \frac{K \times \lambda}{\beta \cos\theta} \quad (1)$$

where: D – particle size (nm); K – constant value (0.9); λ – X-ray wavelength (Å) (1.54060); β – half-width at the maximum peak value (FWHM) (rad); θ – angle of the maximum peak height (rad).

Antimicrobial properties of synthesised silver nanoparticles. The cultures were activated in 10 mL of tryptic soy broth (105459; Merck, Germany) and then incubated at 37 °C for 24 h. Subsequently, 0.1 mL of this culture was transferred onto a Petri dish, and around 15 mL of tryptic soy agar (105458, TSA; Merck, Germany) was added to prepare the medium for the antimicrobial tests. AgNPs were synthesised at 10 and 25 mg·mL^{-1} concentrations, and their antimicrobial activity was assessed using the paper disk method. The nanoparticle solution was prepared with sterile distilled water and subjected to ultrasonic treatment in a water bath for 1 h to ensure a homogeneous distribution. This AgNP solution was then applied to filter paper disks and positioned on the agar plates. A chloramphenicol antibiotic disk (30 µg; Bioanalys, Türkiye) was used as a positive control, while the extract concentration was set at a 1 : 1 ratio for the negative control.

Statistical analysis. The study was conducted in two parallel sets with three replicates each. The obtained microbiological analysis results were analysed using the multivariate analysis of variance (MANOVA) test in the SPSS program, and values below $P < 0.05$ were considered statistically significant.

RESULTS AND DISCUSSION

Properties of silver nanoparticles obtained from *S. officinalis* extract. The AgNP solutions, synthesised from aqueous *S. officinalis* extracts prepared at 20 and 60 °C, exhibited identical colour change times. The 20 and 60 °C extracts displayed maximum peaks at 395 and 410 nm, respectively. Similarly, the peak wavelengths of the spectra for AgNPs synthesised at these temperatures were identified at 360 nm (Figures 1 and 2). The absorbance values of AgNPs ob-

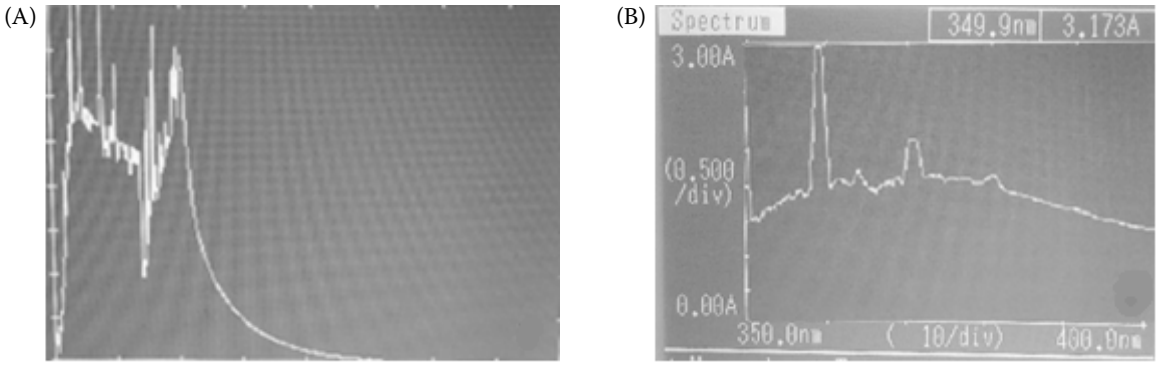

Figure 1. Spectrum graph of (A) sage extract and (B) sage silver nanoparticles solution prepared at 20 °C

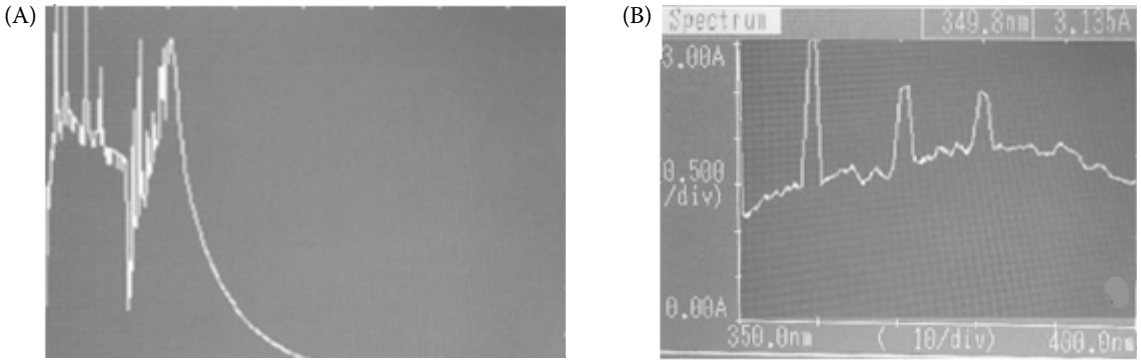

Figure 2. Spectrum graph of (A) sage extract and (B) sage silver nanoparticles solution prepared at 60 °C

https://doi.org/10.17221/4/2024-CJFS

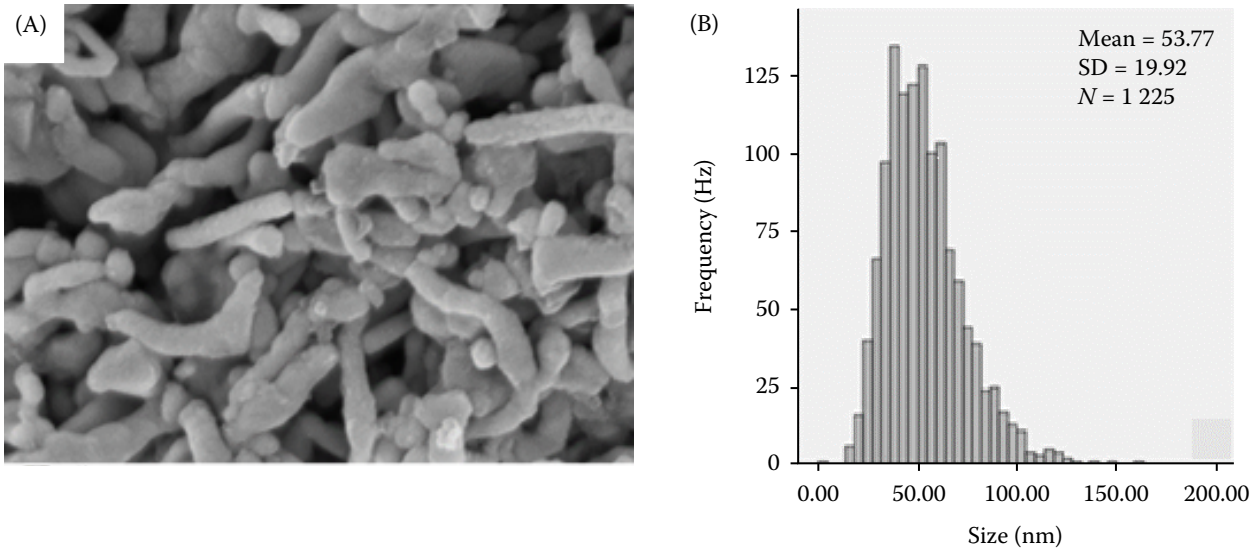

Figure 3. Scanning electron microscopy results of nanoparticles obtained from the extract at 20 °C: (A) 200 000 magnification and (B) histogram graph of nanoparticle size

SD – standard deviation; *N* – number of measured nanoparticles

tained in some studies are in the range of 310–430 nm, and the absorbance values obtained in our study also fall within this range (Sehnal et al. 2019, Okaiyeto et al. 2021, Ödemiş et al. 2022, Takçı et al. 2023).

The sizes and shapes of AgNPs are significantly affected by factors such as reaction temperature, pH, plant components, and metal concentration (Rana et al. 2020; Al-Khattaf 2021). In this particular study, the pH of the sage extract was determined to be 6.6, and the average dimensions of the AgNPs obtained from this extract were investigated using SEM. The mean sizes of AgNPs synthesised from extracts prepared at 20 and 60 °C were measured as 53.77 and 57.08 nm, respectively. Notably, the nanoparticles exhibited a spherical-rod morphology at both temperatures (Figures 3 and 4). Barbinta-Patrascu et al. (2013) used ultrasonic irradiation to obtain sage silver nanoparticles. The morphology (size and shape) of phytosil-

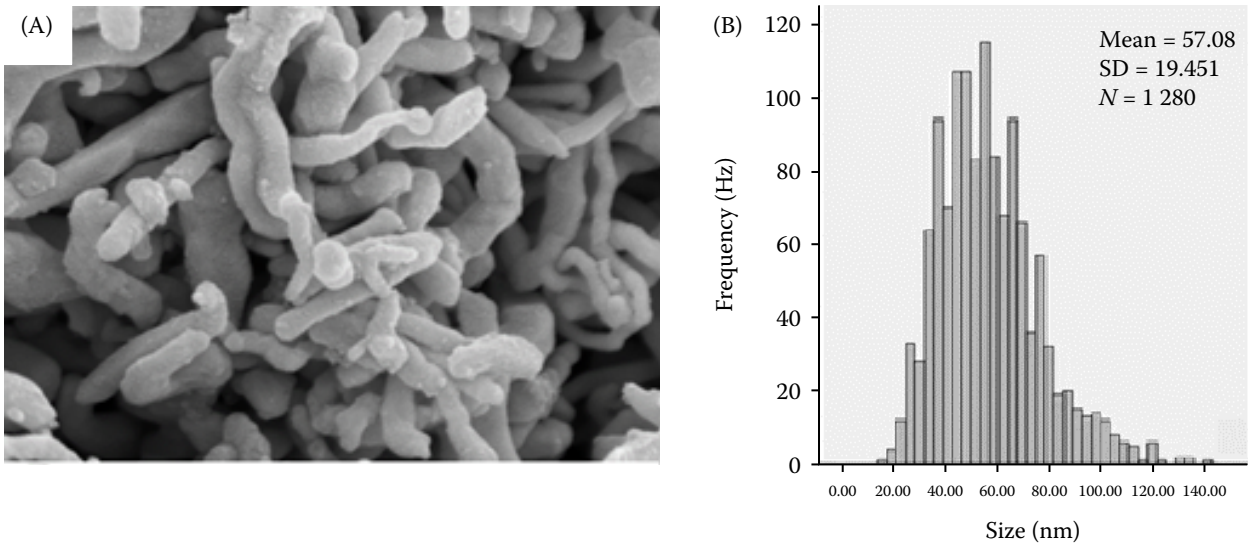

Figure 4. Scanning electron microscopy results of nanoparticles obtained from the extract at 60 °C: (A) 200 000 magnification and (B) histogram graph of nanoparticle size

SD – standard deviation; *N* – number of measured nanoparticles

https://doi.org/10.17221/4/2024-CJFS

ver nanoparticles was evaluated by the SEM, which revealed the formation of spherical phytonanoparticles with a size of less than 80 nm. The present study observed that AgNPs synthesised at 60 °C were slightly larger than those synthesised at 20 °C. Hernandez-Pinero et al. (2016) indicated that both temperature and plant selection impact the size of the resulting AgNPs, with higher temperatures leading to smaller AgNPs forming. Therefore, it may be possible to synthesise AgNPs with a certain diameter range by changing parameters such as different plant species, reaction temperature, and pH.

In a study involving the *S. officinalis* plant, nanoparticle sizes were determined to be 41 nm using TEM, and their shape was observed to be spherical according to SEM (Okaiyeto et al. 2021). The results of the present study are consistent with previous research on biosynthesised AgNPs from various medicinal plants, highlighting the prevalence of spherical-shaped nanoparticles (Sankar et al. 2013; Aldosary and Abd El-Rahman 2019; Pirtarighat et al. 2019; Tailor et al. 2020). Previous studies have emphasised the superior efficacy of spherical-shaped nanoparticles over rod-like or hexagonally-shaped ones. The biological effectiveness of AgNPs is heavily influenced by their size and surface area; smaller nanoparticles possess larger surface areas than larger ones (Zhao et al. 2017).

EDX analysis was performed to determine the elements of AgNPs synthesised from extracts at 20 and 60 °C. EDX nanoparticle results showed strong peaks of silver at 3 eV, while weak peaks outside silver were thought to be primarily due to the sage plant and the carbon tape used during the analysis. The results are given in Figure 5.

Albeladi et al. (2020) reported the silver content of the AgNPs obtained from *S. officinalis* to be 80.47%, and Okaiyeto et al. (2021) reported the silver content of the AgNPs obtained from *S. officinalis* to be 60.97%.

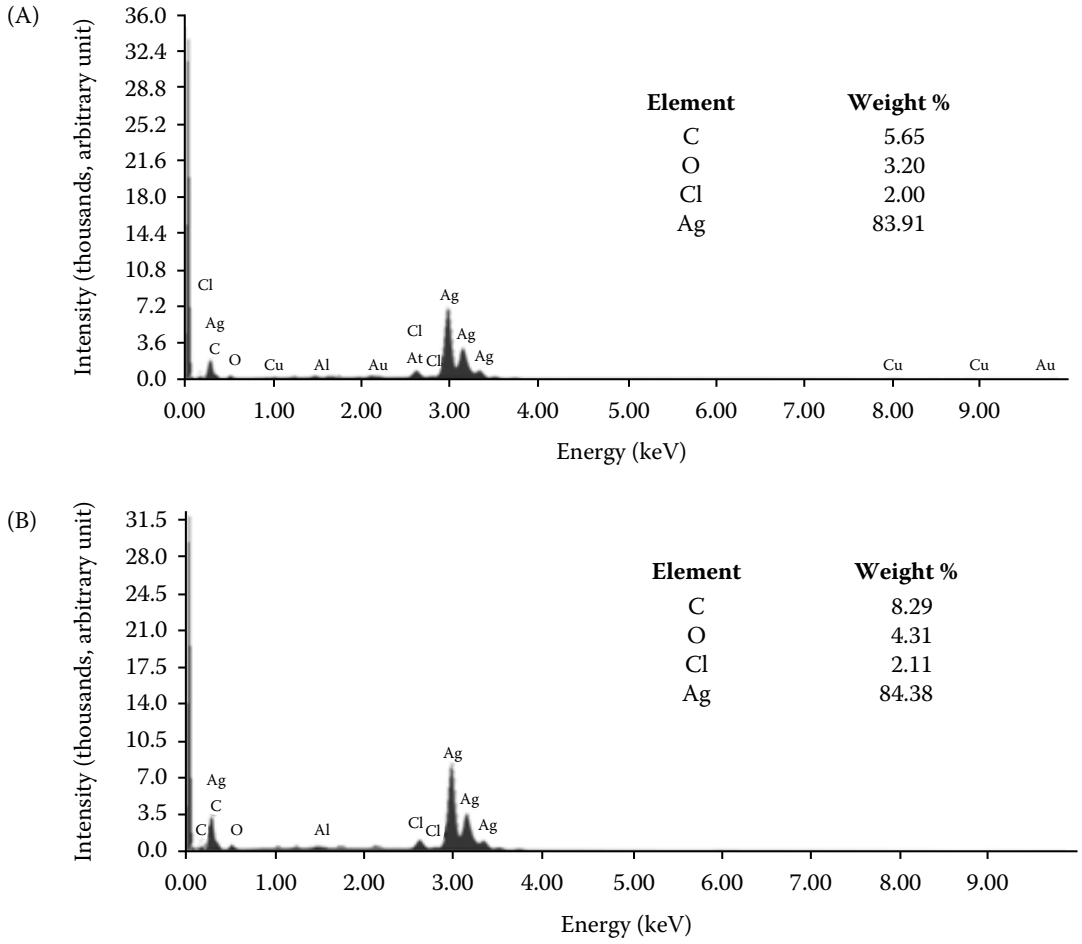

Figure 5. Energy-dispersive X-ray spectroscopy result of the nanoparticles obtained from sage extract at (A) 20 °C and (B) 60 °C

C – carbon; O – oxygen; Cl – chlorine; Ag – silver

https://doi.org/10.17221/4/2024-CJFS

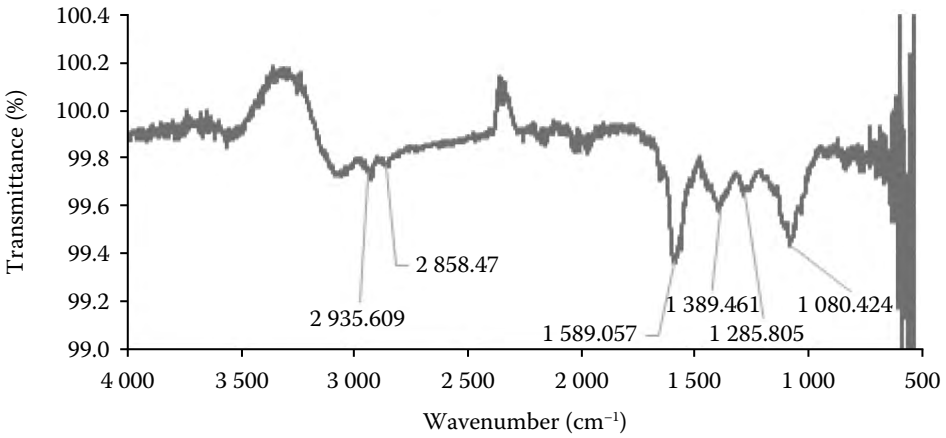

Figure 6. Fourier transform infrared spectrum of the sage extract at 20 °C

Compared to these other studies, the silver content of the nanoparticles obtained in the present study was higher.

The spectrum peaks of the sage extract at a temperature of 20 °C reveal the following vibrational modes: 2 935 cm^{-1} for the C-H stretching band, 2 858 cm^{-1} for C-H stretching (alkanes or secondary amines), 1 589 cm^{-1} for C=C (flavonoids and terpenoids) or C=O (proteins or amide I) stretching vibrations, 1 389 cm^{-1} for the C-N group (aromatic amine group), and 1 080 cm^{-1} for C-O-C or C-O groups (amide-linked carbonyl vibration). Additionally, the spectrum peaks of AgNP's synthesised using this temperature were determined to be 2 156, 2 032, 1 978, 1 595, 1 356, 1 152, and 613 cm^{-1}. Comparing the peaks of sage extract and AgNP, groups C=C, C=O, and C-N are considered effective in nanoparticle formation by reducing silver (Figures 6 and 7).

The spectrum peaks of the extract at a temperature of 60 °C indicate the presence of specific functional groups. The peak at 2 935 cm^{-1} corresponds to the C-H stretching vibration of aliphatic groups. Peaks at 1 589 cm^{-1} may be attributed to C=C vibrations, indicating the potential presence of flavonoids and terpenoids or C=O vibrations, which could be associated with proteins or amide I groups. Furthermore, the peak observed at 1 107 cm^{-1} signifies the presence of C-O-C or C-O groups, which might be related to carbon-oxygen-carbon linkages or amidic carbonyl vibrations. The peak at 1 029 cm^{-1} suggests the presence of carbohydrates.

The spectrum of the silver nanoparticles synthesised from this extract displays distinctive peaks. These peaks are observed at 2 160, 2 017, 1 973, 1 587, 1 343, and 617 cm^{-1}. Comparing the obtained peaks, it is seen that the C=C and C=O groups play a significant role in reducing silver (Figures 8 and 9).

Our results are compatible with the absorbance peak values of the extract obtained from the *S. officinalis* plant used in the Albeladi et al. (2020) and Okaiyeto et al. (2021) studies. The change of peaks confirmed the participation of plant extract compounds in the bio-

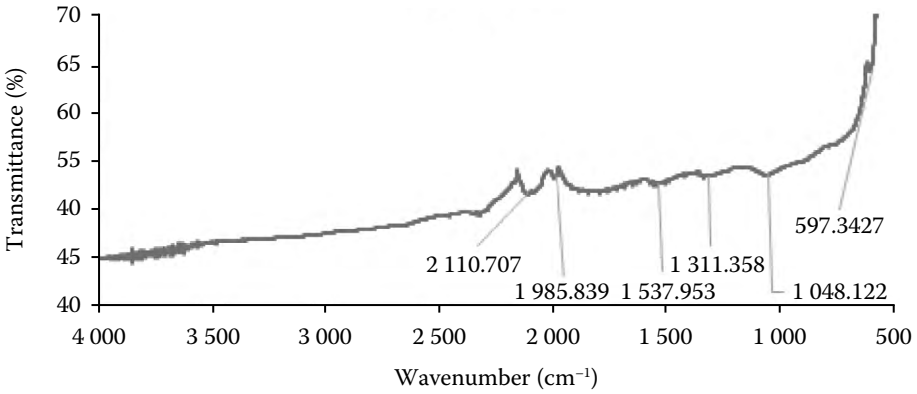

Figure 7. Fourier transform infrared spectrum of the silver nanoparticles obtained from sage extract at 20 °C

https://doi.org/10.17221/4/2024-CJFS

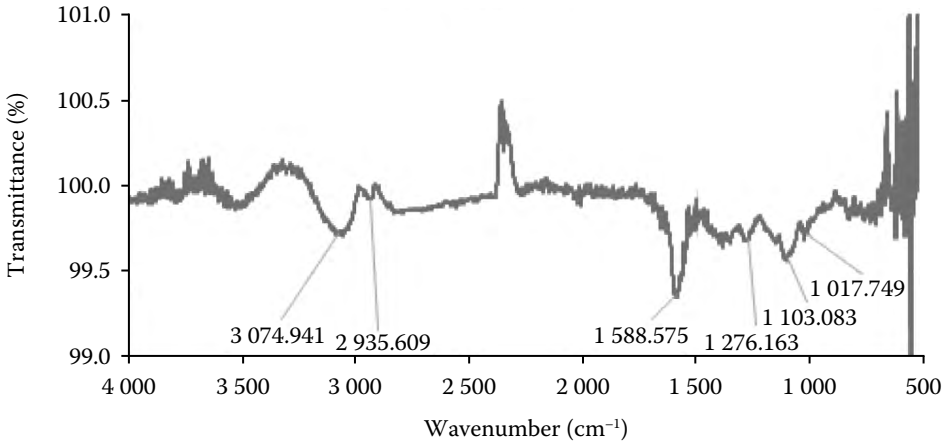

Figure 8. Fourier transform infrared spectrum of sage extract at 60 °C

synthesis of nanoparticles. Therefore, it can be argued that the plant extract compounds containing CH and CO groups are vital in reducing and stabilising NPs. Examining the results of the present study, it was determined that the groups that play a role in nanoparticle formation by reducing silver in sage extracts prepared at 20 and 60 °C were C=C (flavonoids, terpenoids), C=O (amide, protein), C-N (aromatic group), C-O (aromatic group), and C-O-C (amide-bonded carbonyl vibration) (Figures 9 and 10). These functional groups play a significant role as secondary metabolites in reducing silver (Ag) and maintaining nanoparticle formation stability (Paiva-Santos et al. 2021). When comparing our results with those of previous studies, it was observed that the groups involved in Ag reduction were analogous. Simultaneously, these groups remained unaffected by variations in the extraction temperature.

The calculated average crystal size of AgNPs, synthesised from the extract at 20 °C, was 37.15 nm, with the nanoparticles exhibiting a surface-centered cubic structure. The XRD analysis displayed distinct peaks at 38.18, 44.36, 64.48, 77.43, and 81.58° on the 2θ scale. The corresponding Bragg diffraction planes for these angles were identified as (111), (200), (220), (311), and (222), respectively (Figure 10A). The mean crystal size of AgNPs synthesised from the extract at 60 °C was 34.81 nm, and the nanoparticles exhibited a face-centred cubic structure. The peaks at 2θ angles of 37.97, 44.14, 64.30, 77.23, and 81.37° were observed, corresponding to the (111), (200), (220), (311), and (222) diffraction planes, respectively (Figure 10B).

In a similar study conducted with *S. officinalis*, XRD analysis measured the peak points at 2θ angles at 38.09, 44.29, 64.49, 77.43, and 81.64°. Subsequently, applying the Debye-Scherrer equation to the data determined that the resulting nanoparticles exhibited a crystalline and spherical structure, with an average particle size of 42.3 nm (Ödemiş et al. 2022). Geçer (2021) identified the 2θ values as 38.1, 44.3, 64.4, and 77.4° for *Salvia aethiopis*, corresponding to the (111), (200), (220), and (311) reflections of the face-centred

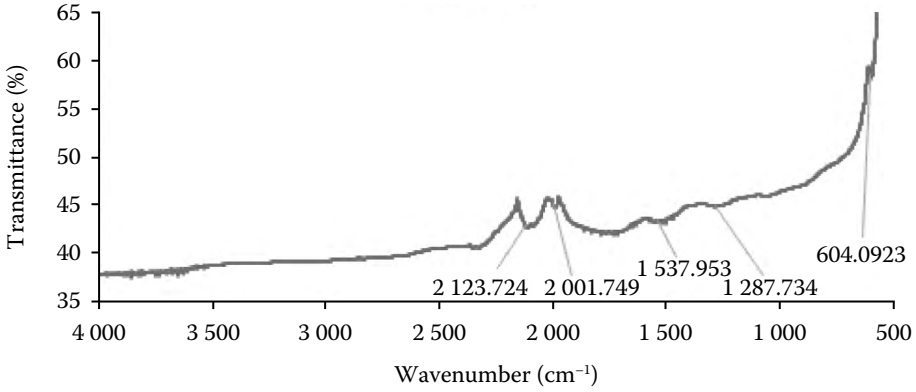

Figure 9. Fourier transform infrared spectrum of silver nanoparticles obtained from sage extract at 60 °C

https://doi.org/10.17221/4/2024-CJFS

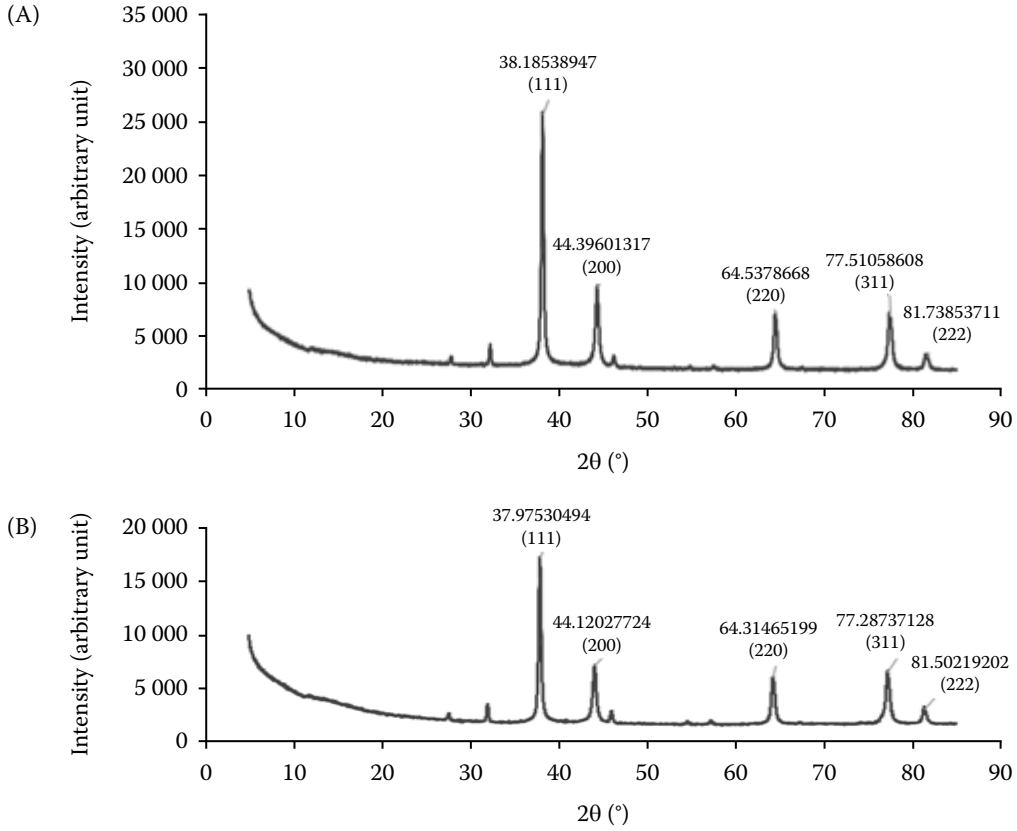

Figure 10. X-ray diffraction result of silver nanoparticles synthesised from sage extract at (A) 20 °C and (B) 60 °C

2θ – angle between transmitted beam and reflected beam

cubic crystalline structure, known as Bragg's reflections. Our findings align with the previous study by demonstrating similar properties in XRD analysis for *S. officinalis*. The present study found that the average crystal sizes of sage nanoparticles obtained from extracts at 20 and 60 °C were 37.15 and 34.81 nm, respectively. The structures of these nanoparticles were determined to be surface-centered cubic. When comparing the crystal sizes of the nanoparticles with the SEM results, the average sizes of the nanoparticles synthesised from extracts obtained at 20 and 60 °C were 53.77 and 57.08 nm, respectively. These values closely aligned with the crystal sizes obtained from XRD analysis. The comparison of our results with previous studies revealed similarities in crystal sizes, diffraction values, and peak points.

Antimicrobial activity of silver nanoparticles obtained from *S. officinalis* extract. The concentrations of bacterial cultures utilised to evaluate the antimicrobial efficacy were 9.9×10^8 CFU·mL^{-1} (CFU – colony forming unit) for *S. aureus*, 3.8×10^8 CFU·mL^{-1} for *L. monocytogenes*, 5.7×10^8 CFU·mL^{-1} for *S.* Typhi, and 6.7×10^8 CFU·mL^{-1} for *E. coli* O157:H7.

The chloramphenicol antibiotic disks, positive control, induced inhibition zones ranging from 19 to 30 mm in diameter on the Petri dishes. The zone of inhibition produced by the sage extract, utilised as the negative control in *S. aureus* and *S.* Typhi cultures, was measured at 8 and 7 mm, respectively. It exhibited negligible efficacy against other bacterial strains (Table 1). AgNPs derived from the extract prepared at 20 °C demonstrated a 9 mm zone of inhibition in the only *S. aureus* culture at a concentration of 10 mg·mL^{-1}. AgNPs synthesised at a 25 mg·mL^{-1} concentration manifested a 7 mm inhibition zone in both *S. aureus* and *S.* Typhi cultures. However, they exhibited limited effectiveness against other bacterial strains. The AgNPs synthesised from the extract at 60 °C exhibited no antimicrobial activity against the four tested bacteria at 10 mg·mL^{-1} concentration. At a concentration of 25 mg·mL^{-1}, these nanoparticles generated a zone of inhibition measuring 7 mm in cultures of *S. aureus, L. monocytogenes*, and *S.* Typhi. In contrast, the AgNPs derived from extracts synthesised at both temperatures did not affect *E. coli* O157:H7. The results showed that two distinct temperature-based sage extracts and the AgNPs syn-

https://doi.org/10.17221/4/2024-CJFS

Table 1. Antimicrobial activity of silver nanoparticles (AgNPs) synthesised from sage

Microorganism	AgNP ($mg \cdot mL^{-1}$)	Zone of inhibition of sage (mm)					
		20 °C			60 °C		
		CA	E	NP	CA	E	NP
Staphylococcus aureus	10	30	ND	9	20	ND	ND
	25	25	8	7	21	8	7
Listeria monocytogenes	10	19	ND	ND	19	ND	ND
	25	19	ND	ND	19	ND	7
Salmonella Typhi	10	21	ND	ND	21	ND	ND
	25	21	ND	7	21	7	7
Escherichia coli O157:H7	10	21	ND	ND	24	ND	ND
	25	22	ND	ND	23	ND	ND

CA – chloramphenicol (30µg); E – extract; NP – nanoparticles; ND – not detected

thesised from these extracts were ineffective against the pathogenic bacteria used in the study. The outcomes of the statistical analysis indicated that the effect of varying concentrations and nanoparticles derived under different extraction temperatures on pathogenic bacteria was deemed insignificant ($P > 0.05$).

Similar to our results, Taghavizadeh Yazdi et al. 2019 reported that AgNPs synthesised from *Salvia leriifolia* revealed inhibition zones measuring 10.5, 10, 9, and 7 mm against *E. coli*, *P. aeruginosa*, *S. aureus*, and *B. subtilis*, respectively. In contrast, Barbinta-Patrascu et al. (2013); Pirtarighat et al. (2019); Tailor et al. (2020); Hatipoğlu (2022); Takçı et al. (2023) exhibited high antibacterial activity against *S.* Typhimurium, *P. aeruginosa*, *S. aureus*, and *E. coli*. The comparatively lower observed antimicrobial activity in this study is hypothesised to be primarily due to the low concentration utilised. Analysis of the results indicated that the obtained nanomaterials exhibit a spherical morphology, are of minute size, and possess a notably high silver content.

AgNPs, owing to their size, bind to cell membrane proteins, thereby catalysing the generation of reactive oxygen species during bacterial growth, causing adverse effects on cells through oxidative stress (Al-Khattaf 2021). The antimicrobial activity attributed to the release of silver ions can be elucidated through various mechanisms, including forming reactive oxygen species, disrupting cellular morphology, inactivating crucial enzymes, DNA condensation, and interference with DNA replication. Direct interaction between AgNPs and bacterial cells disrupts the cell wall and membrane, resulting in the release of cellular contents and eventual cell death. Since the peptidoglycan layer in the cell wall of Gram (–) bacteria is thinner, the cell membrane is damaged more easily (Nayak et al. 2015; Rajeshkumar et al. 2017). As a result, the synthesized AgNPs display discernible antimicrobial activity (Lopes and Courrol 2018; Pallela et al. 2018). However, the results obtained from the present study indicate that nanoparticles derived from *S. officinalis* were ineffective at the concentrations of 10 and 25 $mg \cdot mL^{-1}$ used. Therefore, future investigations might necessitate working with higher inoculum concentrations.

CONCLUSION

Nanoparticles acquired through green synthesis are deemed innovative, given their environmentally friendly nature, cost-effectiveness, and practicality. Therefore, despite the drawbacks of physical and chemical methods, this method is gaining popularity worldwide. The outcomes of this study demonstrate that AgNP can be effectively derived from *S. officinalis*, which is extensively cultivated in America, Asia, and Mediterranean countries. The study revealed that the characteristics of nanoparticles obtained under two different extraction temperatures, as assessed through UV-spectrophotometry, SEM, EDX, FTIR, and XRD, exhibit substantial similarity, with notably high silver content. Notably, synthesising sage metabolites, crucial in reducing silver for nanoparticle synthesis, displayed no variation when using different extraction temperatures. Conversely, the effect of sage extract and AgNPs on pathogenic bacteria employed to ascertain antimicrobial activity fell short of expectations. This will likely impact the ease of conducting studies on nanoparticle synthesis. In the present study, the ex-

https://doi.org/10.17221/4/2024-CJFS

pected level of antibacterial activity not being achieved is thought to be due to the concentration of the AgNPs used despite their high silver content. Within this context, further research is imperative to discern the attributes of nanoparticles that can be derived from plants rich in phenolic substances. Moreover, this study has great economic, environmental and medical significance since herbs and food wastes can be converted into 'green' metallic nanoparticles with high biomedical value.

REFERENCES

Albeladi S.S.R., Malik M.A., Al-Thabaiti S.A. (2020): Facile biofabrication of silver nanoparticles using *Salvia officinalis* leaf extract and its catalytic activity towards Congo red dye degradation. Journal of Materials Research and Technology, 9: 10031–10044.

Aldosary S.K., Abd El-Rahman S.N. (2019): Green synthesis and antibacterial properties of silver nanoparticles of *Lawsonia inermis, Rhamnus frangula, Camellia sinensis* and *Thymus vulgaris* extracts. Journal of Pure and Applied Microbiology, 13: 1279–1284.

Al-Khattaf F.S. (2021): Gold and silver nanoparticles: Green synthesis, microbes, mechanism, factors, plant disease management and environmental risks. Saudi Journal of Biological Sciences, 28: 3624–3631.

Barbinta-Patrascu M.E., Bunghez I.-R., Iordache S.M., Badea N., Fierascu R.-C., Ion R.M. (2013): Antioxidant properties of biohybrids based on liposomes and sage silver nanoparticles. Journal of Nanoscience and Nanotechnology, 13: 2051–2060.

Geçer E.N. (2021): Green synthesis of silver nanoparticles from *Salvia aethiopis* L. and their antioxidant activity. Journal of Inorganic and Organometallic Polymers and Materials, 31: 4402–4409.

Hatipoğlu A. (2022): Green biosynthesis of silver nanoparticles using *Prunus cerasifera pissardii nigra* leaf and their antimicrobial activities against some food pathogens. Czech Journal of Food Science, 40: 383–391.

Hernández-Morales L., Espinoza-Gómez H., Flores-López L.Z., Sotelo-Barrera E.L., Núñez-Rivera A., Cadena-Nava R.D., Alonso- Núñez G., Espinoza K.A. (2019): Study of the green synthesis of silver nanoparticles using a natural extract of dark or white *Salvia hispanica* L. seeds and their antibacterial application. Applied Surfaces Science, 489: 952–961.

Hernández-Pinero J.L., Terrón-Rebolledo M., Foroughbakhch R., Moreno-Limón S., Melendrez M.F., Solís-Pomar F., Pérez-Tijerina E. (2016): Effect of heating rate and plant species on the size and uniformity of silver nanoparticles synthesized using aromatic plant extracts. Applied Nanoscience, 6: 1183–1190.

Kumar P.V., Kala S.M.J., Prakash K.S. (2019): Green synthesis derived Pt-nanoparticles using *Xanthium strumarium* leaf extract and their biological studies. Journal of Environmental Chemical Engineering, 7: 103146.

Lopes C.R.B., Courrol L.C. (2018): Green synthesis of silver nanoparticles with extract of *Mimusops coriacea* and light. Journal of Luminescence, 199: 183–187.

Nayak D., Pradhan S., Ashe S., Rauta P.R., Nayak B. (2015): Biologically synthesised silver nanoparticles from three diverse family of plant extracts and their anticancer activity against epidermoid A431 carcinoma. Journal of Colloid and Interface Science, 457: 329–338.

Nazri M.K.H.M., Sapawe N. (2020): A short review on green synthesis of iron metal nanoparticles via plants extracts. Materials Today: Proceedings, 31: 48–53.

Ödemiş O., Özdemir S., Gonca S., Arslantaş A., Ağırtaş M.S. (2022): The study on biological activities of silver nanoparticles produced via green synthesis method using *Salvia officinalis* and *Thymus vulgaris*. Turkish Journal of Chemistry, 46: 1417–1428.

Okaiyeto K., Hoppe H., Okoh A.I. (2021): Plant-based synthesis of silver nanoparticles using aqueous leaf extract of *Salvia officinalis*: Characterization and its antiplasmodial activity. Journal of Cluster Science, 32: 101–109.

Paiva-Santos A.C., Herdade A.M., Guerra C., Peixoto D., Pereira-Silva M., Zeinali M., Mascarenhas-Melo F., Paranhos A., Veiga F. (2021): Plant-mediated green synthesis of metal-based nanoparticles for dermopharmaceutical and cosmetic applications. International Journal of Pharmaceutics, 597: 120311.

Pallela P.N.V.K., Ummey S., Ruddaraju L.K., Pammi S.V.N., Yoon S.G. (2018): Ultra small, mono dispersed green synthesized silver nanoparticles using aqueous extract of *Sida cordifolia* plant and investigation of antibacterial activity. Microbial Pathogenesis, 124: 63–69.

Pirtarighat S., Ghannadnia M., Baghshahi S. (2019): Green synthesis of silver nanoparticles using the plant extract of *Salvia spinosa* grown *in vitro* and their antibacterial activity assessment. Journal of Nanostructure in Chemistry, 9: 1–9.

Rajeshkumar S., Bharath L.V. (2017): Mechanism of plant-mediated synthesis of silver nanoparticles – A review on biomolecules involved, characterisation and antibacterial activity. Chemico-Biological Interactions, 273: 219–227.

Rana A., Yadav K., Jagadevan S. (2020): A comprehensive review on green synthesis of nature-inspired metal nanoparticles: Mechanism, application and toxicity. Journal of Cleaner Production, 272: 1–25.

Sankar R., Karthik A., Prabu A., Karthik S., Shivashangari K.S., Ravikumar V. (2013): *Origanum vulgare* mediated biosynthesis of silver nanoparticles for its antibacterial and

https://doi.org/10.17221/4/2024-CJFS

anticancer activity. Colloids and Surfaces B: Biointerfaces, 108: 80–84.

Sehnal K., Hosnedlová B., Dočekalová M., Staňková M., Uhlířová D., Tothova Z., Kepinska M., Milnerowicz H., Fernandez C., Ruttkay-Nedecky B., Nguyen H.V., Ofomaja A., Sochor J., Kizek R. (2019): An assessment of the effect of green synthesized silver nanoparticles using sage leaves (*Salvia officinalis* L.) on germinated plants of maize (*Zea mays* L.). Nanomaterials, 9: 1550.

Taghavizadeh Yazdi M.E., Modarres M., Amiri M.S., Darroudi M. (2019): Phyto-synthesis of silver nanoparticles using aerial extract of *Salvia leriifolia* Benth and evaluation of their antibacterial and photo-catalytic properties. Research on Chemical Intermediates, 45: 1105–1116.

Tailor G., Yadav B.L., Chaudhary J., Joshi M., Suvalka C. (2020): Green synthesis of silver nanoparticles using *Ocimum canum* and their antibacterial activity. Biochemistry and Biophysics Reports, 24: 100848.

Takçı D.K., Ozdenefe M.S., Genç S. (2023): Green synthesis of silver nanoparticles with an antibacterial activity using *Salvia officinalis* aqueous extract. Journal of Crystal Growth, 614: 127239.

Zhao Y., Wang Y., Ran F., Cui Y., Liu C., Zhao Q., Gao Y., Wang D., Wang S. (2017): A comparison between sphere and rod nanoparticles regarding their *in vivo* biological behavior and pharmacokinetics. Scientific Reports, 7: 4131.

Received: January 6, 2024
Accepted: April 19, 2024
Published online: May 15, 2024